Journal of Catalysis **204,** 1–10 (2001)
doi:10.1006/jcat.2001.3345, available online at http://www.idealibrary.com on IDEAL®

Influence of Acidic Support in Metallocene Catalysts for Ethylene Polymerization

V. I. Costa Vayá,* P. G. Belelli,† J. H. Z. dos Santos,‡ M. L. Ferreira,‡ and D. E. Damiani†,[1]

*Universidad de Valencia, Valencia, Spain; †Planta Piloto de Ingeniería Química, Plapiqui (UNS-CONICET), Camino la Carrindanga Km 7 (8000), Bahía Blanca, Argentina; and ‡Instituto de Quimica, Universidad Federal de Rio Grande do Sul, Porto Alegre, Brasil

Received September 14, 2000; revised March 9, 2001; accepted July 29, 2001

We studied a ZSM-5 zeolite as metallocene support for ethylene polymerization. We transformed the Na-ZSM-5 into H-ZSM-5. After the cation exchange, the zeolite was calcined at three different temperatures. Characterization of the material indicated that by means of the calcination procedure it is possible to produce dealuminization with an increase in extraframework aluminum (EFAL). We prepared zirconocene-supported catalysts on zeolitic supports using two preparation methods. The higher activity was observed with the zirconocene supported on ZSM-5 pretreated at 900°C. We think that the dealuminization process generates an increase in EFAL. This EFAL is responsible for the higher activity.

Key Words: **ZSM-5 zeolite support; supported-metallocene catalyst; ethylene polymerization.**

INTRODUCTION

There are numerous papers dealing with metallocene/methylaluminoxane (MAO) soluble systems in olefin polymerization (1, 1a, 1b, 1c, 2, 3). These systems are characterized by high productivity and produce polymers with special properties, like a narrow molecular weight distribution. Commercial use of metallocene catalysts in industrial gas reactors requires its heterogenization on inorganic solids. Moreover, supported-metallocene catalysts require a smaller amount of MAO than soluble systems to achieve high activity.

For these reasons the heterogenization of metallocene catalysts is necessary if the drop-in from Ziegler-Natta to metallocenes in industrial gas processes is the objective. Silica and alumina have been studied as inorganic supports (4–6). Others supports used were zeolites (7). The latter are crystalline aluminosilicates with a framework structure in three-dimensional arrangement of tetrahedral TO_4 (T = usually Si^{4+}, Al^{3+}). These arrangements form channels and cavities with specific dimensions; thus the catalytic sites can be entrapped in the cavity. These supports present a well-defined pore structure with an extremely narrow pore size distribution.

These materials are used like supports in oligomerization (8), copolymerization (9–11), and homopolymeri zation of olefins. Woo *et al.* (12) studied ethylene polymerization on NaY zeolite previously treated with MAO or TMA (trimethylaluminum) and posterior fixation of Cp_2ZrCl_2. They observed a high decrease in activity compared with the soluble catalyst, but an increase in molecular weight and melting point of the polymer. The same authors said that termination and chain transfer reaction rates are slower than those of the homogeneous catalyst. The presence of active sites in cavities produces steric hindrance for deactivation reactions. Woo *et al.* think that the spherical shape of some zeolite cavities forces linear MAO to round up inside the supercage, which is known to be a favorable configuration for the formation of active sites. In a later paper the same authors (13) studied propylene polymerization with other catalytic systems ($EtInd_2ZrCl_2$). In this case the supports were MCM-41 and VPI-5 zeolites. They found that the activities are important in both cases, but the molecular weight, melting point, and *mmmm* fraction of polypropylene (PP) were slightly superior with VPI-5 than MCM-41 and also higher than the PP obtained with a homogeneous system. The VPI-5 has channels of smaller diameter than MCM-41 and for this reason the properties of PP were slightly superior. The conclusion was that steric hindrance prevents the active sites from forming binuclear complexes between metallocenes. Also, it permits the formation of stable sites metallocene/MAO, and leads to high activity in propylene polymerization. The metallocene in the regular cylindrical pores could be more stereoselective than the homogeneous $EtInd_2ZrCl_2$.

Results reported by Altomare and co-workers (14) show that reduction of the bulk Si/Al mole ratio from 27 to 5.7 in different zeolites was accompanied by a marked decrease in polymer productivity by supported metallocenes on these zeolites. They think that the dealumination process could

[1] To whom correspondence should be addressed. Fax: 54-291-4861600. E-mail: ddamiani@plapiqui.edu.ar.

0021-9517/01 $35.00

partially create mesopores in the zeolite framework, which are supposed to accommodate the polymer chain growing on the active site. They report an increase in the molecular weight of polypropylene and polyethylene obtained with these supported metallocene catalysts.

An interesting point of view was investigated by Marques *et al.* (15). They used two zeolites: HY and mordenite (MOR). The results of ^{27}Al-NMR confirmed the removal of aluminum atoms from the lattice during calcination due to the increase in Si/Al ratio (bulk). IR studies showed a decrease in the Brønsted/Lewis acid sites with dealumination. Both zeolites have a high Si/Al ratio. The productivity in ethylene polymerization with supported catalysts is lower than with the corresponding homogeneous system, but a significant increase in MW with no change in the polydispersion of PE was observed. Marques *et al.* think that the dominant factor in making a zeolite a suitable support is the concentration of framework aluminum atoms.

In a recent work Ciardelli *et al.* (11) reported a small decrease in activity of a metallocenic catalyst supported on HY zeolite when the Si/Al ratio was high, comparing it with homogeneous catalyst in ethylene polymerization. Molecular weight was increased in the same way as activity. Zeolites pretreated with MAO have higher productivity than those not treated.

The studies reported in recent literature use NaY zeolites or mesoporous silica MCM-41 (7) as supports for metallocenes. The present article aims to study H-ZSM-5 zeolite as a support for metallocene catalysts to be used in ethylene polymerization. The zeolite was thermally pretreated before interaction with MAO or zirconocene. We studied the effect of dealuminization in ethylene polymerization activity. We think that an adequate acidic support could be important in improving productivity. Previous reports from our group found an increase in activity when $AlCl_3$ (a Lewis acid) was added to the $EtInd_2ZrCl_2$/MAO system in propylene polymerization.

EXPERIMENTAL

Materials

Cp_2ZrCl_2 (Aldrich) and MAO (Witco), 10 wt% in toluene, were used without further purification and were manipulated in a N_2 atmosphere. Ethylene polymerization grade was decontaminated using MnO/Al_2O_3 and activated 13X molecular sieve columns to retain water and oxygen J. T. Baker HPLC (water 0.006%) toluene was dehydrated with 13X molecular sieves.

Support

Na-ZSM-5 was the initial zeolite support with Si/Al = 24.3 (Na form, powder, Chemie Uetikon AG, Switzerland). This kind of zeolite has an intermediate pore size with a 10-membered ring pore opening (16). These materials exhibit high intrinsic acidic strength with high thermal stability. The most interesting characteristic is their tridimensional pore system.

The initial support was treated with a 2 M NH_4Cl solution at 90°C with agitation for 5 h (cation exchange). Then the material was washed and centrifuged three times with distilled water. The NH_4-ZSM-5 obtained was dried at 110°C for 14 h and then calcined at 400°C for 4 h. In the last step, water and ammonia were eliminated. After these treatments the support has an acid form, H-ZSM-5 (ZSM5-400). A fraction of the latter material was separated and calcined at two higher temperatures: 700°C (ZSM5-700) and 900°C (ZSM5-900). It is known that treatment of zeolites at high temperature produces dealuminization without structure collapse depending on the thermal stability of zeolite (16). This process generates the elimination of aluminum from the framework and increases the content of extraframework aluminum (EFAL) (15, 16).

X-Ray powder diffraction, ^{29}Si-NMR, and FTIR spectroscopy of adsorbed pyridine were used to characterize the supports. Infrared spectroscopy is a useful method for providing information on surface properties and on the way reactions or treatments modify them. Changes in spectra yield information about the surface and how the molecules are adsorbed. The treatment with pyridine was done to investigate the changes in the relative number of Brønsted and Lewis acid sites at the surface of different zeolites (16). The sample was maintained at 100°C and finally saturated with pyridine by directing the N_2 flow through a pyridine saturator. This adsorption was maintained for 90 min. Then the zeolite was flushed with N_2 for 2 h at the same temperature to remove weakly adsorbed pyridine. The FTIR spectra were collected at room temperature.

Catalyst Preparation

Two types of supported catalysts were prepared.

Type 1. The metallocene, Cp_2ZrCl_2, was directly deposited on zeolite (ZSM5-400 or ZSM5-900). Zirconocene impregnation was done by contacting the zeolite (500 mg) with a toluene solution containing a known amount of Cp_2ZrCl_2 (20 mg), under N_2 atmosphere at 75°C with agitation for 0.5 h. The resulting solid was washed three times and then dried in N_2. The final catalyst was maintained in hexane solution. These catalysts are named Cp_2ZrCl_2/ZSM5-400 and Cp_2ZrCl_2/ZSM5-900.

Type 2. The zeolite was previously pretreated with MAO before zirconocene impregnation. The solid was prepared by impregnating zeolite (500 mg) with MAO (1.7 ml) at 50°C for 90 min, in N_2 atmosphere with agitation. Then the solid was washed three times with toluene and dried in a N_2 atmosphere. The zirconocene impregnation was done as described for Type 1 catalysts.

TABLE 1

Catalysts Prepared

Catalyst	Support	% Zr
Cp_2ZrCl_2/ZSM5-400	ZSM5-400	0.97
Cp_2ZrCl_2/MAO/ZSM5-400	ZSM5-400	0.93
Cp_2ZrCl_2/ZSM5-900	ZSM5-900	0.61
Cp_2ZrCl_2/MAO/ZSM5-900	ZSM5-900	0.55

These catalysts are named Cp_2ZrCl_2/MAO/ZSM5-400 and Cp_2ZrCl_2/MAO/ZSM5-900.

Characterization of Catalysts

The zirconium content of catalysts was determined with a spectrometric method (17). A Shimadzu UV/Visible-160A spectrometer with a quartz cell (1-cm width) was used. In Table 1 are summarized the nomenclature of prepared catalysts and zirconium content (% Zr).

We conducted X-ray photoelectron spectroscopy (XPS) studies on three of the prepared catalysts: Cp_2ZrCl_2/ZSM5-400, Cp_2ZrCl_2/MAO/ZSM5-400, and Cp_2ZrCl_2/ZSM5-900. We evaluated mainly the catalyst without MAO on its surface because the others will present extra Al from MAO species anchored on the zeolite surface. The Si/Al ratios obtained by this method are only from the zeolite support used in the prepared catalysts. The results for Cp_2ZrCl_2/MAO/ZSM5-400 are presented to evaluate the changes due to the presence of MAO.

X-Ray-induced photoelectron spectra were taken with an Alvac PHI 5600 Esca System (Physical Electronics), using monochromatic Al$K\alpha$ radiation (1486.6 eV). Acquisition was carried out at room temperature in high-resolution mode (0.1-eV step, 23.5-eV pass energy) for the Si 2p, Al 2p, and Zr 3d regions. The samples were mounted as thin films on an adhesive copper tape in a glove box, introduced into a transfer chamber, and then evacuated to 10^{-6} Torr in 90 min using a turbomolecular pump. During data collection, an ion-getter pump kept the pressure in the analysis chamber under 10^{-9} Torr. Takeoff angles (angle between the surface plane and the irradiator) of 45° and 75° were used to control the sampling depth in the XPS experiment. For each of the reported X-ray photoelectron spectra, an attempt has been made to deconvolute the experimental curve into a series of peaks representing photoelectron emission from atoms in different chemical environments. These peaks are described as a mixture of Gaussian and Lorentzian contributions to take instrumental error into account together with the characteristic shape of photoemission peaks. All binding energy values were charge referenced to Au 4$f^{7/2}$ at 84.0 eV. XPS experiments were done at two different angles. At 45° the results obtained correspond to the catalyst surface, while at 75° the information obtained is from a depth near 5 nm.

The XRD spectra were obtained with a Philips PW1710 diffractometer with Cu anode and a graphite monochromator, at 45 kV and 30 mA.

Polymerization

Polymerization was carried out in a 100-ml stainless-steel reactor operated in continuous mode at 50°C using 50 ml of dry toluene. The catalyst solution was introduced into the reactor by syringe. The polymer was washed with a mixture of EtOH/HCl, filtered, and dried until constant weight was obtained. Polymer samples were analyzed by means of intrinsic viscosity [η] in trichlorobenzene at 135°C to determine the viscosity average molecular weight (M_v) by means of the Mark–Howink equation. The melting point of polymers was determined by differential scanning calorimetry (DSC). The DSC equipment was a Perkin Elmer 7 with a Pyris 1.0 Beta Version acquisition system.

The homogeneous polymerization of ethylene was done in a continuous way, at 1 atm in 300 ml of solvent. [Zr] was 2.27×10^{-05} M, Al/Zr was 2000 (in the reactor), and a preactivation step of 30 min with Al(MAO)/Zr = 1500 was done. The polymerization time was 1 h and the reaction temperature was 50°C. The results (in terms of activity) were the same with and without the preactivation step.

RESULTS AND DISCUSSION

Support

The X-ray diffraction analyses indicate that zeolites have high crystallinity (Figs. 1–3). For the three samples the spectra are completely defined with narrow peaks in the 2θ range. The structural features of the zeolites produced by calcination at different temperatures showed no significant changes. This indicates that no changes in the internal structure of zeolites occurred. An increase in peak intensity

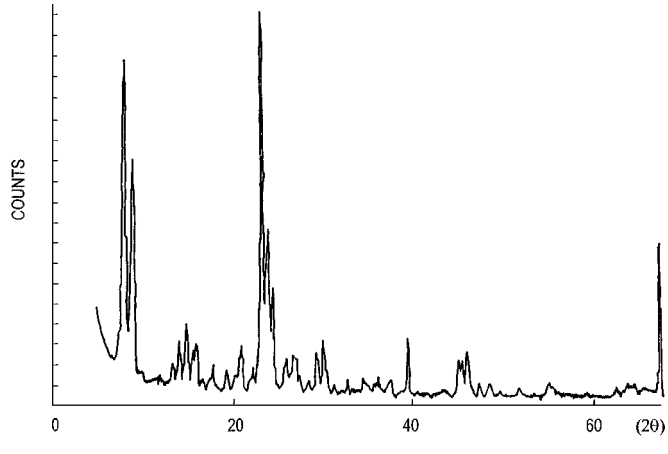

FIG. 1. X-Ray powder diffraction spectra of ZSM5-400 zeolite.

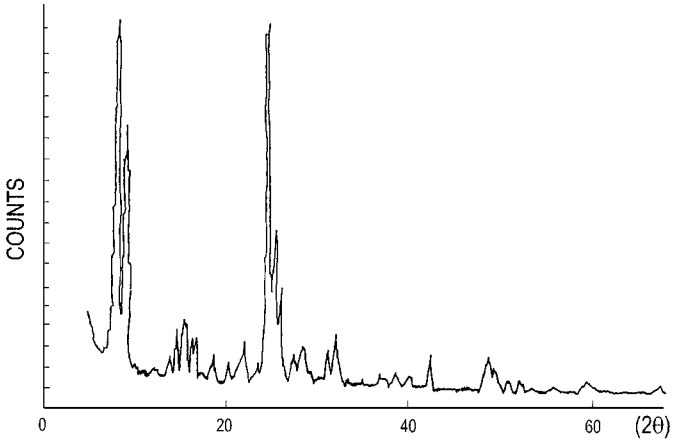

FIG. 2. X-Ray powder diffraction spectra of ZSM5-700 zeolite.

at 8.045 and 8.925 angles was observed when the zeolite was calcined at 700°C. No changes were observed between ZSM5-700 and ZSM5-900 samples. Analyzing the former change with a pattern provided by the X-ray software leads one to think that the increase in calcination temperature produces a zeolite with a smaller amount of aluminum in the lattice. A similar result was obtained by Corma *et al.* (18) who reported that an increase in calcination temperature produced MCM-41 samples with a higher degree of dealuminization. These results are in agreement with several papers and the known process of dealuminization (15). The XRD pattern of ZSM5-400 can be related to an XRD standard that corresponds to a formula per unit cell expressed in Table 2. The ZSM5-700 sample represents a spectrum between both standards shown in Table 2.

FTIR analysis showed that a gradual decrease in the OH bands in the region 3400–3700 cm^{-1} takes place when the calcination temperature is increased. The FTIR spectrum

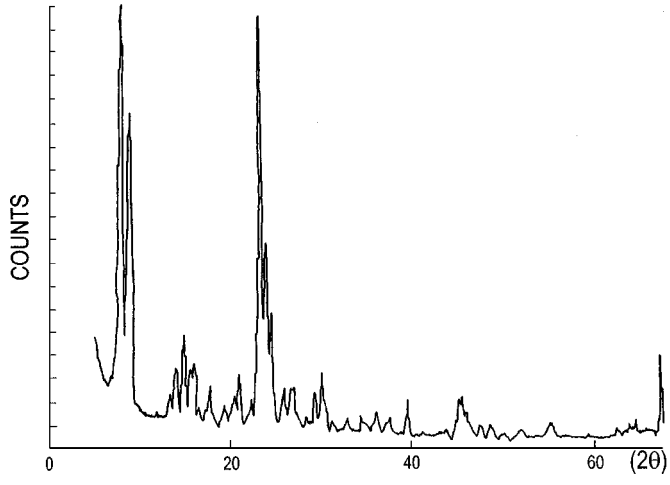

FIG. 3. X-Ray powder diffraction spectra of ZSM5-900 zeolite.

TABLE 2

Characterization of Treated Zeolites

Sample	Formula of unit cell	Lewis[a]/Brønsted[b]	Si/Al[c]
Na-ZSM5	—	—	24.3
ZSM5-400	$H–Al_2O_3–SiO_{21}$	0.91	40
ZSM5-700	↓	0.39	40
ZSM5-900	$H_{0.32}Al_{0.32}Si_{95.68}O_{192}$	2	75

[a] Determined from 1450 cm^{-1} band.
[b] Determined from 1545 cm^{-1} band.
[c] Determined by ^{29}Si-NMR.

of ZSM5-700 sample reveals a decrease in the band corresponding to silanols with different interactions and water occluded in the cavities and channels during synthesis. An important decrease in this band was observed in the FTIR spectrum of ZSM5-900 sample (results not shown). The band at 3747 cm^{-1} is not altered by the presence of pyridine, indicating that the OH groups giving rise to this band are not acidic (19). This band slightly increases in ZSM5-700 spectra and then decreases again in ZSM5-900 support. These results are in agreement with those given in Ref. (19).

The FTIR study was used to determine the relative amount of Brønsted and Lewis acid sites by means of pyridine adsorption on these sites. Pyridine chemisorbs on Brønsted sites as pyridinium ions, giving rise to a band at 1545 cm^{-1}. Pyridine adsorption on Lewis sites produces a band at 1450 cm^{-1} (16). The bands centered at 1440 cm^{-1} correspond to both Lewis and Brønsted acid sites. To some authors (16) IR spectroscopy is not a good technique for quantification of the Lewis/Brønsted acid site ratios. Others like Rosenthal *et al.* (20) found that the extinction coefficients for these Lewis-pyridine and Brønsted-pyridine bands were equal. We tried to explain our results taking into account a recent work by Emeis (21). From this analysis and our results we obtained a Lewis/Brønsted ratio for the zeolites. We use this method to qualitatively (not quantitatively) determine the change in this ratio in the pretreated zeolites. The spectra of zeolite either treated with pyridine or untreated are shown in Figs. 4–6. Both bands mentioned above are clearly seen. Their intensity ratio depends on the sample examined. The Lewis/Brønsted ratio increases with calcination temperature (see Table 2). This effect is due to changes in the nature and number of acid sites. The thermal treatment produces a change from aluminum into the framework (Brønsted acid) to aluminum extraframework, giving a Lewis acid site. The ZSM5-900 material presents a split of the 1450 cm^{-1} band into two new bands: one of them is at 1441 cm^{-1} while the other is at 1445 cm^{-1}. Two kinds of Lewis acid sites would be present in this support. Parry (25) found a similar result in alumina support. The ZSM5-700 sample has a decrease in this ratio with respect to ZSM5-400. A simple explanation for these

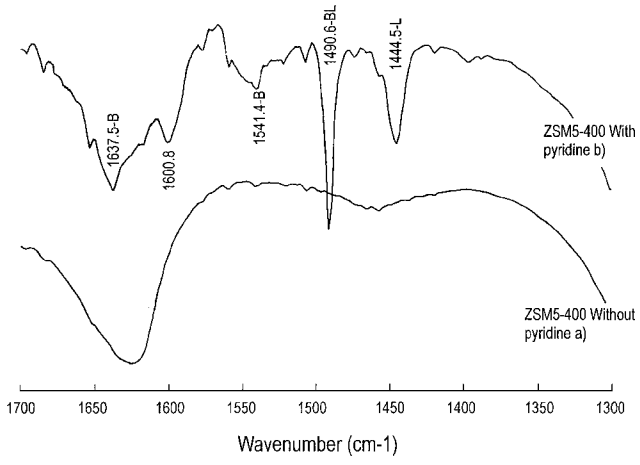

FIG. 4. FTIR spectra (a) before and (b) after adsorption of pyridine on ZSM5-400 zeolite.

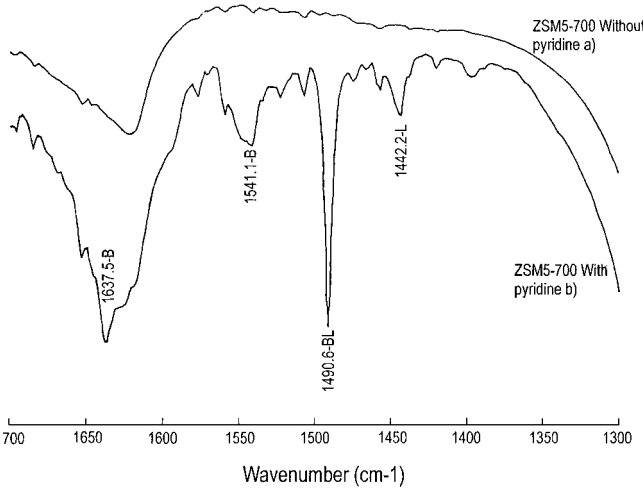

FIG. 5. FTIR spectra (a) before and (b) after adsorption of pyridine on ZSM5-700 zeolite.

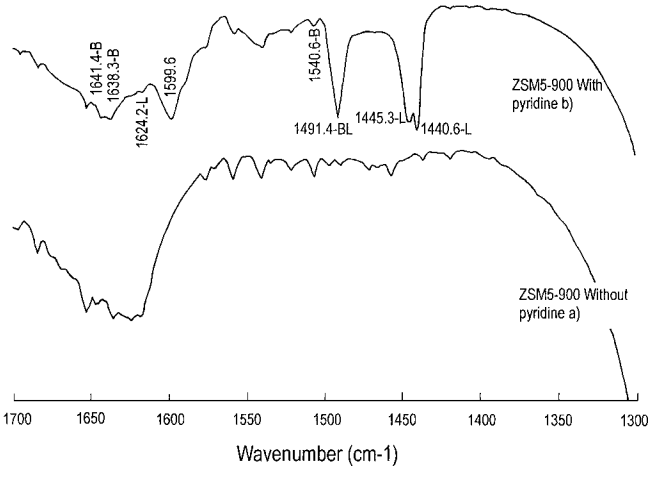

FIG. 6. FTIR spectra (a) before and (b) after adsorption of pyridine on ZSM5-900 zeolite.

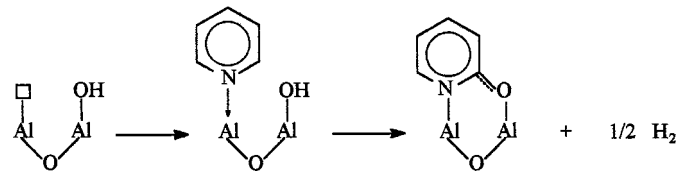

SCHEME 1. Possible pyridone species found on both Lewis and OH sites.

results is difficult to find. Knözinger and co-workers (22–24) observed an IR band centered at 1640 cm^{-1} on partially dehydroxylated alumina that contained both Lewis sites and OH groups (Scheme 1). This band was assigned as pyridone because this species has a stretching band at 1634 cm^{-1}. In a more recent investigation carried out by Corma *et al.* (18) the results found were explained by considering that the large amount of Lewis acid sites would be due to the EFAL formed having a lower degree of polymerization as Al_2O_3. They are forming Al–O–Si bonds and not Al–O–Al bonds in high concentration. Taking into account these experiences we can postulate that an intermediate calcination temperature (700°C) is sufficient to generate a change in crystalline structure as shown by the X-ray results, but is not enough to produce dealuminization. We think that a great amount of aluminum migrates to the zeolite surface and forms a layer of aluminum oxide. Pyridone species can be present on aluminum oxide because an increase in the 1638 cm^{-1} band is observed (Scheme 1) after pyridine is adsorbed. A reduction in the intensity of pyridine coordination band (1444.5 cm^{-1}) occurs because a minor amount of Lewis acid sites exists as a consequence of a higher degree of polymerization of the EFAL. The IR spectra of this sample show an increase in the 1638 cm^{-1} band, compared with the sample ZSM5-400, as well as a reduction in the Lewis acid band. The 1600 cm^{-1} band, generally assigned to hydrogen-bonded pyridine, disappeared in ZSM5-700 (25). Therefore the support does not present weak Brønsted sites. These sites would be responsible for pyridone formation (see Scheme 1).

The ^{29}Si-NMR spectrum of zeolites showed poor resolution, but it is possible to deconvolute the peaks (Figs. 7–9). From these spectra we obtained the Si/Al ratios listed in Table 2. The results indicate that the ZSM5-400 and ZSM5-700 samples have the same Si/Al ratio. Using 400 and 700°C as calcination temperatures, we obtained an increase in this ratio compared with the initial material (Si/Al = 24.3). The dealuminization process has been achieved with higher efficiency in ZSM5-900 than in ZSM5-400 or ZSM5-700 samples. This result agrees with the explanation given for the low Lewis/Brønsted acid site ratio in the ZSM5-700 sample. For this reason no apparent dealuminization occurs in the latter and this is proved because of the unchanged Si/Al ratio (bulk).

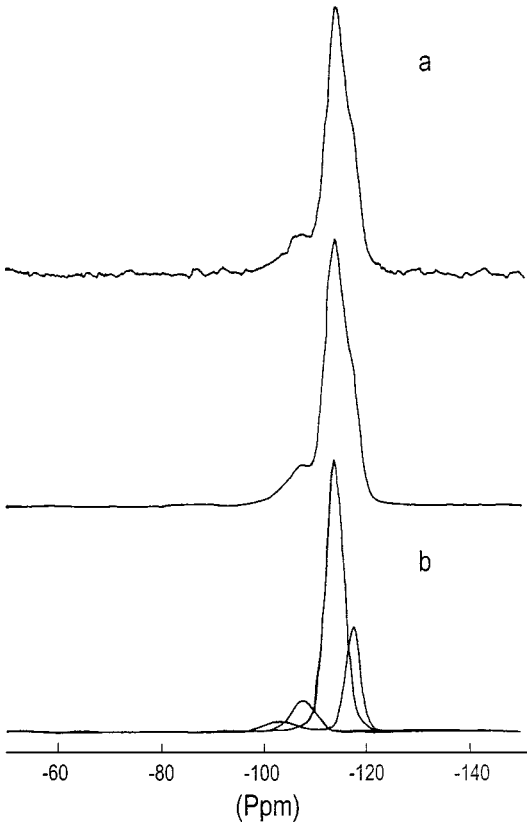

FIG. 7. (a) ^{29}Si-NMR image of ZSM5-400 zeolite and (b) with deconvoluted peaks.

XPS

The results obtained from XPS studies are summarized in Table 3. More details are given in Tables 4–6.

Two Si signals are found: Si (bulk) and Si (surface). The reported XPS values found for ZSM5 (102.5 eV) are in the published range for different zeolites: 102.55 (NaY), 102.45 (CaX), and 102.0 (NaX) (26). Only one species of Al is detected in Cp_2ZrCl_2/ZSM5-400. With the MAO-modified catalyst, Cp_2ZrCl_2/MAO/ZSM5-400, two different forms are found: one at higher energy (73.7 eV) similar to that found for the zeolite without MAO, and another at 72.5 eV, probably resulting from the interaction with the zeolite surface or the metallocene. This species seems to be located at the surface, since its concentration increases 17 to 28% when the sampling moves to the surface (75° to 45°).

When we analyze Zr, the presence of two signals are due to spin-orbit coupling of the 3*d* electrons of Zr: ca. 183 eV (3*d* 5/2) and 185 eV (3*d* 3/2). The binding energies of Cp_2ZrCl_2 (in the measure at 75°) are 180.85 and 183.19 eV. In MAO/SiO_2, two species are found at 182.89 and 185.67 eV (71%) and 184.49 and 186.15 eV (29%),

TABLE 3

XPS Ratios of Prepared Catalysts

Catalyst	Angle	Zr/Al	Zr/Si	Si/Al
Cp_2ZrCl_2/ZSM5-400	45°	0.41	0.016	25.6
	75°	0.49	0.017	28.7
Cp_2ZrCl_2/MAO/ZSM5-400	45°	0.073	0.108	0.675
	75°	0.074	0.119	0.623
Cp_2ZrCl_2/ZSM5-900	45°	0.40	0.039	10.3
	75°	0.69	0.043	16.7

TABLE 4

XPS Data on Cp_2ZrCl_2/ZSM5-400

Element	Angle	BE (eV)	FWHM (eV)	%
Si	45°	102.5	2.05	87
		101.0	2.40	13
	75°	102.5	2.03	84
		101.5	2.40	16
Al	45°	73.61	2.60	100
		—	—	—
	75°	73.6	2.70	100
		—	—	—
Zr[a]	45°	182.4–184.7	2.04–2.02	100
	75°	182.2–184.6	2.09–2.06	100

[a] BE of both peaks of the doublet.

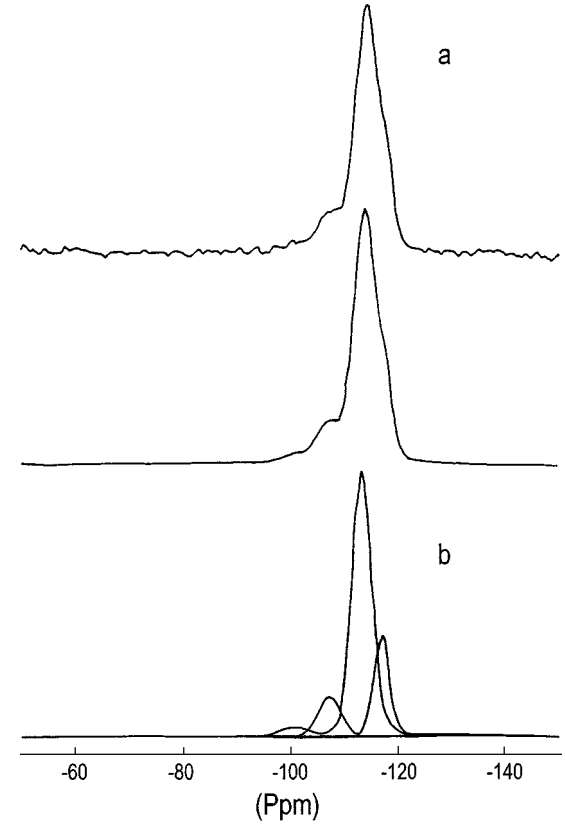

FIG. 8. (a) ^{29}Si-NMR image of ZSM5-700 zeolite and (b) with deconvoluted peaks.

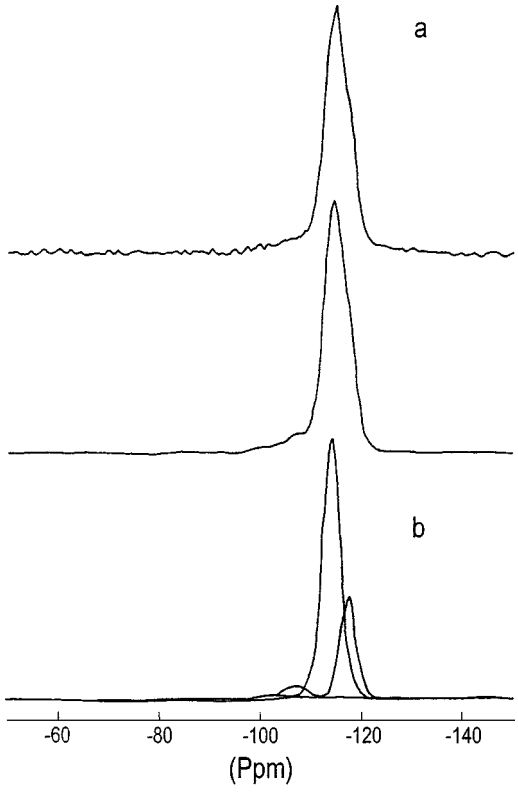

FIG. 9. (a) ^{29}Si-NMR image of ZSM5-900 zeolite and (b) with deconvoluted peaks.

respectively. Some authors reported that the Zr binding energy in Cp_2ZrCl_2 is 181.7 eV (3*d* 5/2). Treatment of this zirconocene with MAO affords a new species with a binding energy of 182.4 eV (27). The supported metallocene suffers an increase in binding energy, suggesting that the Zr is electrodeficient. Treating the zeolite with MAO generates a different species of Zr, with a binding energy at 181.2 eV. In the case of Cp_2ZrCl_2/ZSM5-900 the spectrum (at 75° angle) shows that Al has a low level of detection. In the of case of Cp_2ZrCl_2/MAO/ZSM5-400

TABLE 5

XPS Data on Cp_2ZrCl_2/MAO/ZSM5-400

Element	Angle	BE (eV)	FWHM (eV)	%
Si	45°	102.5	2.23	80.5
		100.4	2.90	19.5
	75°	102.5	2.10	82.5
		100.9	2.50	17.5
Al	45°	73.9	1.93	72.0
		72.5	2.40	28.0
	75°	73.7	1.92	82.5
		72.6	2.22	17.5
Zr[a]	45°	182.5–184.8	1.87–2.03	82.7
		181.2–183.3	2.40–1.80	17.3
	75°	182.3–184.7	2.22–2.04	100

[a] BE of both peaks of the doublet.

TABLE 6

XPS Data on Cp_2ZrCl_2/ZSM5-900

Element	Angle	BE(eV)	FWHM (eV)	%
Si	45°	102.5	2.11	85
		101.0	2.50	15
	75°	102.5	2.10	78
		101.1	2.50	22
Al	45°	73.9	2.70	100
		—	—	—
	75°	73.7	2.60	100
		—	—	—
Zr[a]	45°	181.9–184.4	2.39–2.10	100
	75°	181.9–184.2	2.41–2.10	100

[a] BE of both peaks of the doublet.

the doublet near Al 2*p* is an Au signal. In both systems, Cl is detected. When Cp_2ZrCl_2/ZSM5-400 is considered, the metallocene seems to be uniformly distributed. In the case of Cp_2ZrCl/ZSM5-900, it locates mainly inside, but not uniformly. The Zr loading in the latter is lower than in Cp_2ZrCl_2/ZSM5-400 or Cp_2ZrCl_2/MAO/ZSM5-400 (see Table 1). However, the Zr/Si ratio obtained from the signal taken at 45° increases from 0.016 in Cp_2ZrCl_2/ZSM5-400 to 0.039 in Cp_2ZrCl/ZSM5-900 (see Table 3).

Since the XPS experiments give information coming from two different depths, it is possible to speculate on the way the different elements are distributed through the zeolite structure. The Si/Al ratio of Cp_2ZrCl_2/ZSM5-400 catalyst increases when the angle of analysis is enlarged. A similar result was found in Cp_2ZrCl_2/ZSM5-900, but the increase is more important. Therefore, this ratio is lower for both catalysts when the XPS signal is taken at 45°. This result is in agreement with those obtained in the FTIR study. Both groups of data show the increase in the extraframework Al when the calcination temperature is higher. The Si/Al ratio increases 60% from the surface to the inner part of the solid. In the high temperature-treated zeolite a larger amount of Al is found near the surface. When the treatment temperature is lower the increase is less. The Si/Al ratio varies in Cp_2ZrCl_2/MAO/ZSM5-400 due to MAO fixed at the preparation step. An important decrease in this ratio is observed because of the amount of fixed Al due to MAO. The Si/Al ratio decreases 8% in the bulk of the support.

Figures 10 and 11 show the spectra of Cp_2ZrCl_2/ZSM5-900 and Cp_2ZrCl_2/MAO/ZSM5-400.

Zr/Al and Zr/Si ratios are also obtained from XPS results. From the Zr/Al ratio, Cp_2ZrCl_2/ZSM5-400 and Cp_2ZrCl_2/ZSM5-900 catalysts show similar results when the surface is analyzed. Taking into account the higher Zr loading in Cp_2ZrCl_2/ZSM5-400 it can be concluded that the zirconocene would be preferentially located inside the zeolite. In Cp_2ZrCl_2/MAO/ZSM5-400 the zirconocene would be fixed mainly onto the exterior surface. However, there is an important increase in the Zr/Al ratio in

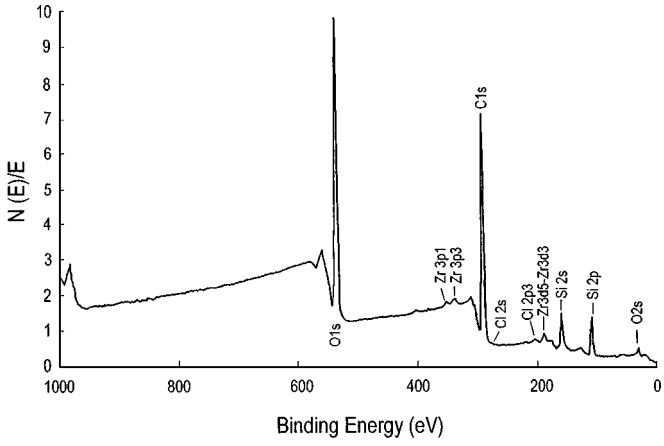

FIG. 10. X-Ray photoelectron spectrum of Cp_2ZrCl_2/ZSM5-900.

Cp_2ZrCl_2/ZSM5-900 when the signal at 75° is analyzed (near 72%) compared with that obtained at 45°. We can say that this is due to the decreased concentration of structural Al because of dealuminization; although another explanation is that the zirconocene is placed in the cavities, besides the surface. Therefore the EFAL would not be blocking the pores of the zeolitic structure. Zr/Si ratio is increased in Cp_2ZrCl_2/ZSM5-400 and Cp_2ZrCl_2/ZSM5-900 when the XPS signal analyzed is taken at 75°. The decrease in the relative amount of Si produces in Cp_2ZrCl_2/ZSM5-900 an increase in the Zr/Si ratio, compared with Cp_2ZrCl_2/ZSM5-400, although the Zr loading is lower. A slight increase in Zr/Si was observed when we analyzed deeper.

The results are different for Cp_2ZrCl_2/MAO/ZSM5-400. The Si/Al ratio decreases because of the extra Al from fixed MAO. This ratio remains unchanged when we analyze deeper. Therefore the distribution of MAO seems to be uniform, at least near the surface. Cp_2ZrCl_2/MAO/ZSM5-400 shows a higher Zr/Si than Cp_2ZrCl_2/ZSM5-400

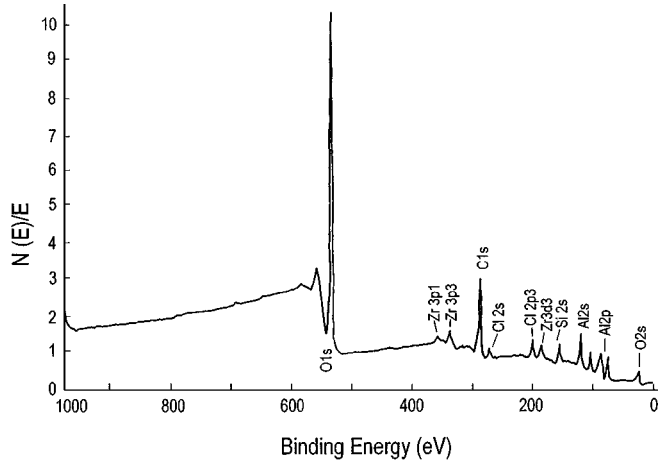

FIG. 11. X-Ray photoelectron spectrum of Cp_2ZrCl_2/MAO/ZSM5-400.

and Cp_2ZrCl_2/ZSM5-900, being the amount of supported zirconocene near that found in Cp_2ZrCl_2/ZSM5-400.

When we consider the results of ^{29}Si-NMR the bulk Si/Al ratio cannot be considered as a tool to correlate with activity. The bulk Si/Al ratio increases to 75 in the sample treated at 900°C (Cp_2ZrCl_2/ZSM5-900), but the XPS analysis shows that the Si/Al surface ratio is very much lower (10.3–16.7). The same takes place in Cp_2ZrCl_2/ZSM5-400 but in this case the difference is not as great.

Polymerization

From the characterization of the three zeolites we decided to test ZSM5-400 and ZSM5-900 as supports in ethylene polymerization with Cp_2ZrCl_2 catalyst, since these supports showed different characteristics. We used two preparation methods. In the first, the zirconocene was directly fixed on zeolite support, while in the second, the surface was previously impregnated with MAO. The prepared catalysts have different Zr loadings depending on the zeolite surface. When ZSM5-400 was used, large amounts of Zr were fixed independently of the preparation method. These results are in agreement with the higher OH concentration available for MAO or zirconocene anchoring. The zirconocene can irreversibly deactivate over supports with high OH concentration during adsorption (25). Zr loading is lower in ZSM5-900. The results of polymerization are listed in Table 7. In all cases studied in this report, we found an increase in activity when the metallocene was fixed on zeolite surface compared with a homogeneous system. Our results are in agreement with the results of Rieger and Janiak (28). According to them, although Cp_2ZrCl_2/MAO is a known polymerization catalyst, there is still a lack of knowledge concerning certain factors that influence the polymerization, one being the concentration dependence. At constant Al (MAO)/Zr ratio, productivity critically depends on zirconium concentration. It is accepted that in diluted solutions the homogeneous complex with its higher activity dominates the polymerization profile. There is a limit for lowering the Zr concentration. A decrease from $[Zr] = 10^{-5}$ M to 2×10^{-6} M under otherwise unchanged reaction conditions leads from good to no observable

TABLE 7

Ethylene Polymerization Results Obtained with Supported Catalysts

Catalyst	$[Zr] \times 10^6$	Al/Zr	[Al]	Activity[a]
Cp_2ZrCl_2	22.7	2000	0.033	250
Cp_2ZrCl_2/ZSM5-400	27.0	1481	0.04	1961
Cp_2ZrCl_2/MAO/ZSM5-400	13.2	3030	0.04	4045
Cp_2ZrCl_2/ZSM5-900	13.1	3030	0.04	5707
Cp_2ZrCl_2/MAO/ZSM5-900	19.8	2016	0.04	6535

[a] Expressed in kg PE/mol Zr/h/atm.

productivity. We observed this under in our conditions at low [Zr] concentrations (10^{-6} M, 40°C, continuous, Al/Zr = 1500–2000). To retain a comparable productivity for lower [Zr], the Al/Zr has to be raised to 7000. Extremely high Al/Zr ratios of 150,000 or even 500,000 for the record productivity of 500,000 kg PE/mol Zr · h · bar are associated with low [Zr](10^{-7} or 10^{-8} M). As a consequence, we can reduce the amount of MAO needed for activation. The productivity was better when the zirconocene was impregnated over the zeolite pretreated with MAO. This result has been obtained in many reports in the literature when SiO_2 has been used as support (4). When MAO is impregnated on the zeolite surface the OH groups react with MAO, preventing its interaction with the zirconocene. Also, an increase in activity is observed when catalysts prepared by the same method with different supports are compared. In this case an increase in the acidity of the zeolite surface leads to higher productivity. These results are in agreement with previous results obtained by our group in ethylene polymerization with a soluble system (29). An increase in activity was observed when an adequate amount of $AlCl_3$ (Lewis acid) was added to the $EtInd_2ZrCl_2$/MAO system in ethylene polymerization. Taking into account these results, the larger amount of active sites would be located on the surface of the zeolite, where a higher amount of extraframework Al is present, whereas Cp_2ZrCl_2/ZSM5-400 has the active sites in the channels.

From the published literature we find similar results when an increase in the Si/Al ratio is achieved. According to data reported by Marques *et al.* (15) NaM zeolite has the highest activity, with Si/Al = 5.3. The rest of the investigated zeolites have a lower Si/Al ratio (framework). These authors consider this factor very important with respect to the increase in productivity. However, we think that another essential factor is the extraframework aluminum. In the case mentioned above, the Si/Al ratio is very small with respect to our data. It is important not to exceed the content of aluminum because a new decrease in productivity can occur. For this reason an increase in the extraframework aluminum diminishes the activity. In the present work the Si/Al ratio is higher than that used by Marques *et al.* (15). For this reason an enhancement of extraframework aluminum concentration produces an increase in activity. Other results are found in agreement with our results. Rahiala *et al.* (7) reported that the increase in support acidity produces enhancement of activity. Catalysts prepared on zeolites with bulk Si/Al = 32 have better productivity than mesoporous silica MCM-41. It is important to have some surface Lewis acidity to improve activity. The zeolites are characterized by a large range of acidity from which to choose a good support for metallocene catalyst. It is possible to find a support with adequate Lewis acidity. In our case, the increase in calcination temperature of ZSM-5 zeolite resulted in dealuminization (from Si/Al = 40 to Si/Al = 75). The higher concentration of extraframework Lewis acid sites is a result of dealuminization, Si/Al at the surface being an important parameter to correlate with activity.

TABLE 8

Characterization of PE Obtained with Supported Catalysts

Catalyst	$[\eta]$	M_v^a	Melting point (°C)
Cp_2ZrCl_2	2.15	137.000	—
Cp_2ZrCl_2/ZSM5-400	2.13	135.200	134.6
Cp_2ZrCl_2/MAO/ZSM5-400	3.12	228.800	134.5
Cp_2ZrCl_2/ZSM5-900	1.67	96.700	127.8
Cp_2ZrCl_2/MAO/ZSM5-900	2.41	160.300	135.6

[a] Converted with Mark–Howink constants: $k = 0.000406$, $\alpha = 0.725$.

From Table 8 we can conclude that the molecular weight of polyethylene (calculated as viscosimetric with the Mark–Howink equation) decreases or is maintained when the zirconocene is placed directly on the support and increases when the support is pretreated with MAO. The increase is higher for the zeolite treated at lower temperature. In the case of the zeolite treated with MAO at higher temperature, the activity is 50% higher but the molecular weight decreases if we compare Cp_2ZrCl_2/MAO/ZSM5-400 and Cp_2ZrCl_2/MAO/ZSM5-900 (see Table 8). In this case, it seems that the propagation constant to termination constant ratio has changed as a consequence of changes in the electrophilicity of Zr. However, we must point out that the molecular weights could be even higher because the polyethylene could contain long-chain branching (LCB) and the LCB concentration could be different. In this case, the molecular weight calculated for linear polyethylene (using Mark–Howink) is not correct. The viscosity of the materials changes, as does the melting point, especially for the polymer obtained with the more acidic surface (Cp_2ZrCl_2/ZSM5-900), and these values are absolute and do not depend on a calculation method, as molecular weight.

Evidently, surface acidity plays a role in the control of the molecular weight (viscosity) of polyethylene. To be sure about the termination reactions on these supported catalysts, more studies must be done, especially about the structure of the obtained materials. To avoid being too speculative, we support the idea of a connection between the surface acidity and molecular weight of polyethylene in a nonspecific way. It is clear that more acidity implies more activity (see Table 7 of the paper), but the correlation is more complex in terms of the molecular weight. Perhaps changing the electrophilicity of Zr arises in new termination reactions besides the transfer to monomer ethylene (improved β-H termination reactions in ethylene polymerization), and therefore the molecular weight decreases or is maintained using more acidic supports. The final molecular weight would be a compromise between propagation and transfer reactions.

The viscosity of polyethylene decreases for Cp_2ZrCl_2/ZSM5-900, compared with soluble catalyst, and remains unchanged for Cp_2ZrCl_2/ZSM5-400 (Table 8). This can be correlated with the higher zeolite surface acidity for Cp_2ZrCl_2/ZSM5-900 (see Table 4). For this catalyst the activity is higher, too (see Table 7). This higher surface acidity influences the MAO impregnated onto it. The activities for Cp_2ZrCl_2/ZSM5-900 and Cp_2ZrCl_2/MAO/ZSM5-900 are closer.

CONCLUSION

The characterization of pretreated zeolites has been useful in understanding the results obtained with metallocene-supported catalysts in ethylene polymerization. Using XPS as an additional tool to FTIR proved essential in understanding the changes in Lewis/Brønsted acidity with calcination temperatures of the zeolites.

The Si/Al ratio in zeolites (bulk) (obtained by ^{29}Si-NMR) seems no to be as important as the surface Si/Al ratio (obtained by XPS). The productivity in ethylene polymerization can be correlated with the increase in surface acidity due to high calcination temperatures, although the Si/Al (bulk) increases. The migration of Al from inside to outside the frame is the main factor. The presence of MAO before impregnation with zirconocene is very important in achieving high activity and high molecular weight of the polymer. MAO on the surface is affected by the acidity of the surface and the changes in the Si/Al molar ratio at the surface.

ACKNOWLEDGMENTS

We acknowledge the Consejo Nacional de Investigaciones Científicas y Técnicas (CONICET) and the Universidad Nacional del Sur (UNS) for their financial support. We thank Professor Raúl Lobo (Delawere University) for the ^{29}Si-NMR spectra and G. Massimiliani and G. Goizueta (Polymer Group-PLAPIQUI) for the polymer viscosity measurements. We acknowledge Professor Marcelo Villar (Polymer Group-PLAPIQUI) for helpful advice on the molecular weight considerations of polyethylene obtained with metallocenes.

REFERENCES

1. Kaminsky, W., and Steiger, R., *Polyhedron* **7**, 2375 (1988).
1a. Scheirs, J., and Kaminsky, W. (Eds.), "Metallocene-based polyolefins." Wiley, London, 1999.
1b. Gladysz, J. A., *Chem. Rev.* **100**, 1167 (2000).
1c. Coates, G. W., *Chem. Rev.* **100**, 1223 (2000).
2. Kaminsky, W., *Catal. Today* **20**, 257 (1994).
3. Hlatky, G. G., *Chem. Rev.* **100**, 1347 (2000).
4. Soga, K., Kim, H. J., and Shiono, T., *Macromol. Chem. Phys.* **195**, 3347 (1994).
5. Sacchi, M. C., Zucchi, D., Tritto, I., and Locatelli, P., *Macromol. Chem. Phys.* **16**, 581 (1995).
6. Semikolenova, N., and Zakharov, V. A., *Macromol. Chem. Phys.* **198**, 2889 (1997).
7. Rahiala, H., Beurroies, I., Eklund, T., Hakala, K., Gougeon, Trens, P., and Rosenholm, J. B., *J. Catal.* **188**, 14 (1999).
8. Van Looveren, L. K., De Vos, D. E., Vercruysee, K. A., Geysen, D. F., Janseen, B., and Jacobs, P. A., *Catal. Lett.* **56**, 53 (1998).
9. Michelotti, M., Altomare, A., Ciardelli, F., and Roland, E., *J. Mol. Catal. A* **129**, 241 (1998).
10. Ko, Y. S., Seo, T. S., Hong, D. S., and Woo, S. I., *in* "Metallorganic Catalysts for Synthesis and Polymerization" (W. Kaminsky, Ed.), p. 369. Springer-Verlag, Berlin, 1999.
11. Ciardelli, F., Altomare, A., and Michelotti M., *in* "Metallorganic Catalysts for Synthesis and Polymerization" (W. Kaminsky, Ed.), p. 359. Springer-Verlag, Berlin, 1999.
12. Woo, S. I., Ko, Y. S., and Han, T. K., *Macromol. Chem. Phys.* **16**, 489 (1995).
13. Ko, Y. S., Han, T. K., and Woo, S. I., *Macromol. Chem. Phys.* **17**, 749 (1995).
14. Michelotti, M., Arribas, G., Bronco, S., and Altomare, A., *J. Mol. Catal. A* **152**, 167 (2000).
15. Marques, M. F., Henriques, C. A., Monteiro, J. L. F., Menezes, S. M. C., and Coutinho, *Macromol. Chem. Phys.* **198**, 3709 (1997).
16. Nagy, J. B., Boudart. P. Hannus, I., and Kiricsi, I., *in* "Synthesis, Characterization and Use of Zeolitic Microporous Materials" (Z. Kónya and V. Tubak, Eds.), p. 20 (1998).
17. Snell, F. D., Snell, C. T., and Snell, C. A., "Colorimetric Methods of Analysis," p. 334 (1959).
18. Corma, A. V. Fornés, Navarro, M. T., and Pérez-Pariente, J., *J. Catal.* **148**, 569 (1994).
19. Tanable, K., Misono, M., Ono, Y., and Hattori, H., *Stud. Surf. Sci.* **51**, 142 (1989).
20. Rosenthal, D. J., White, M. G., and Parks, G. D., *AIChE J.* **33**, 336 (1987).
21. Emeis, C. A., *J. Catal.* **141**, 347 (1993).
22. Knözinger, H., and Stolz, H., *Fortschr. Kolloide Polym.* **55**, 16 (1971).
23. Ghorbel, A., Hoang-Van, C., and Teichner, S. J., *J. Catal.* **33**, 123 (1974).
24. Knözinger, H., Krietenbrink H., Müller, H. D., and Schulz, W., *in* "Proceedings, 6th International Congress on Catalysis, London, 1976" (G.C. Bond, P. B. Wells, and F. C. Tompkins, Eds.), p. 183. Chem. Soc., London, 1977.
25. Parry, E. P., *J. Catal.* **2**, 371 (1963).
26. Barr, T. L., "Modern ESCA: The Principles and Practice of X-Ray Photoelectron Spectroscopy," p. 25. CRC Press, Boca Raton, FL, 1994.
27. Paul. G., Gassmann, M., and Callstrom, *J. Am. Chem. Soc.* **109**, 7875 (1987).
28. Rieger, R., and Janiak, C., *Ang. Makromol. Chem.* **215**, 35 (1994).
29. Belelli, P. G., Ferreira, M. L., and Damiani, D. E., *Macromol. Chem. Phys.* **201**, 1458 (2000).